

# Exploiting the pyramid WFS gain using a deformable lens as an NCPA corrector

M. Bergomi<sup>\*a,b</sup>, M. Quintavalla<sup>c\*</sup>, D. Magrin<sup>a,b</sup>, S. Bonora,<sup>c</sup>  
R. Ragazzoni<sup>a,b</sup>, C. Arcidiacono<sup>a,b</sup>, E. Pinna<sup>b,d</sup>

<sup>a</sup> INAF - Osservatorio Astronomico di Padova, Vicolo dell'Osservatorio 5, 35122 Padova, Italy

<sup>b</sup> ADONI - Laboratorio Nazionale di Ottica Adattiva

<sup>c</sup> CNR-IFN - Istituto di Fotonica e Nanotecnologie, via Trasea 7, 35131 Padova, Italy

<sup>d</sup> INAF - Osservatorio Astrofisico di Arcetri, Largo Enrico Fermi 5, 50125 Firenze, Italy

## ABSTRACT

Pyramid wavefront sensors are widely used in adaptive optics systems, due to their advantages in terms of sensitivity with respect to other wavefront sensors such as the Shack-Hartmann. However, especially in extreme adaptive optics applications, Non-Common Path Aberration (NCPAs) cause image distortions that can hinder the scientific throughput. NCPAs are usually corrected introducing offsets on the pyramid closed-loop control systems, but the consequent increase in the size of the star image on the pyramid pin leads to a decrease in sensitivity that compromises the aforementioned advantages. In principle, these offsets can be counter-balanced by introducing an active optical element in the wavefront sensing channel, recovering the full sensitivity of the pyramid. In this framework, we are studying the capability of Multi-Actuator deformable Lenses to recover such NCPAs. We present in this paper the result obtained on the test-bench that has been realized at CNR-IFN Institute in Padova, with the collaboration of INAF-Padova, aiming at the NCPAs correction by the means of a multi-actuator deformable lens inserted in the sensing path, in order to recover the optimal working conditions and the ideal magnitude gain of the pyramid.

**Keywords:** Deformable lens, Pyramid WFS, NCPA, Adaptive Lens, PZT bimorph

## 1. INTRODUCTION

Pyramid wave-front sensors [1] (P-WFSs), coupled with adaptive secondary mirrors, can nowadays be considered the preferred combination for AO systems in large telescopes, starting from the results obtained since 2010 at the Large Binocular Telescope [2]. The main advantage of the P-WFS, when compared for instance to the Shack-Hartmann WFS (SH-WFS), is the fact that the pyramid sensitivity increases during the loop closure, since the PSF on the tip of the pyramid gets smaller [3]. However, this gain, and consequently the achievable performance, can be reduced if the PSF of the reference star degrades [4]. In an astronomical instrument, where the light is commonly split between the scientific path and the WFS arm, NCPAs between the two paths, depending on poor relative alignment, mechanical flexures and thermal differential effects are one of the main aspects of PSF degradation [5][6][7][8][9], introducing, in particular, low-order aberrations. Since the main focus is the improvement of the scientific camera performance, to deliver a PSF with a high strehl, the PSF reaching the WFS has a lower SR depending on the NCPA entity, and thus the P-WFS cannot be exploited at its best. The technique proposed to solve the NCPAs issue, already presented in [10], is to insert a corrector, such as the Multi-Actuator deformable Lens (MAL), to compensate the low order aberrations in the sensing path, thus delivering a high-strehl PSF also on the pin of the pyramid and obtain on both the sensing and the scientific channels the best achievable performances.

We present in this paper the latest laboratory results, where calibrated aberrations (NCPA) were artificially introduced and a MAL, located in the sensing arm, was used to compensate them, while the main adaptive optics loop is working, thus maximizing the scientific image sharpness. In order to have a more robust measurement and comparison, a SH-WFS sensor was also located on the scientific path and the wavefront value was minimized.

---

\* maria.bergomi@ inaf.it

In Section 2 the MAL is presented, in Section 3 we describe the general concept of application, in Section 4 we illustrate the test-bench setup to demonstrate the feasibility of such a concept and in section 4 we present the obtained results.

## 2. THE MULTI-ACTUATOR DEFORMABLE LENS

The MAL (shown in Figure 2 left) belongs to the category of bimorph piezoelectric deformable elements and has been developed at CNR-Institute of Photonics and Nanotechnology of Padova, Italy. It is composed by two thin (150  $\mu\text{m}$ ) N-BK7 optical windows, filled with transparent mineral oil matching the refractive index of the glass, connected to two piezoelectric rings with 18 actuators, which are located outside the clear aperture of the lens. The upper window is free to move, while the lower window is glued at the border to a rigid aluminum ring, as depicted in Figure 2 right. The clear aperture of the lens can vary from 10 mm (the one used in our test-bench) up to 25 mm.

The actuation of the lens allows a wavefront modulation up to the 4th order of Zernike polynomials with a relatively fast time response (frequency up to 400 Hz, rise-time 2 msec). Each actuator can be independently actuated applying voltages between -125 and +125 Volts, allowing to generate (and thus correct) aberrations up to the 4<sup>th</sup> radial order. The achievable stroke varies for different aberrations and the maximum achievable strokes are shown in Table 1, where can be also noticed that astigmatism can achieve about 10 waves ( $\lambda=632.8$  nm) PtV. The voltage percentage used to obtain a minimum residual WFE on the lens, meaning the correction of internal aberrations, is about 10%. Another characteristic worth mentioning is the fact that its control electronics is very compact and light-weighted and that it can be controlled through a USB connection to a laptop.

The MAL has proved its potentiality in the past few years in other fields and applications, such as microscopy or ophthalmic in vivo application [11] [12][13] and more recently in the astronomical field, for small telescopes [14].

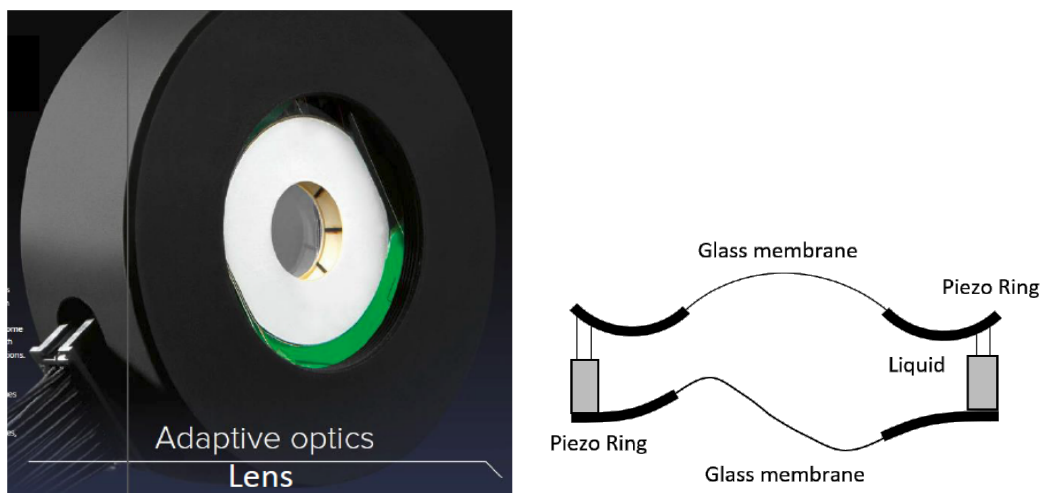


Figure 1: Picture and conceptual functioning scheme of the Multi Actuator Adaptive optic lens.

Aberration	Zernike order	PtV( $\mu\text{m}$ )
Tilt	$Z_{11}, Z_{1-1}$	3
Defocus	$Z_{20}$	3.8
Astigmatism	$Z_{22}, Z_{2-2}$	7.7
Coma	$Z_{31}, Z_{3-1}$	2.2
Trefoil	$Z_{33}, Z_{3-3}$	2.9
Spherical Ab.	$Z_{40}$	0.5
Secondary Ast.	$Z_{42}, Z_{4-2}$	0.75
Quadrifoil	$Z_{44}$	1.2

Table 1: Aberrations and their maximum stroke obtainable with the MAL. Astigmatism can reach a very high stroke compared to other aberrations, due to the actuators configuration.

## 3. CONCEPT OF OPERATIONS

A common optical scheme of an astronomical instrument is reported in Figure 1. A dichroic beam splitter separates the light between the scientific path and the sensing arm, introducing differential aberrations between the two paths.

As mentioned earlier, the scientific channel performance is commonly optimized to deliver a PSF with a high Strehl ratio at the expenses of the P-WFS arm. However, the better the SR on the pin of the pyramid, the better the AO correction, the better also the scientific image.

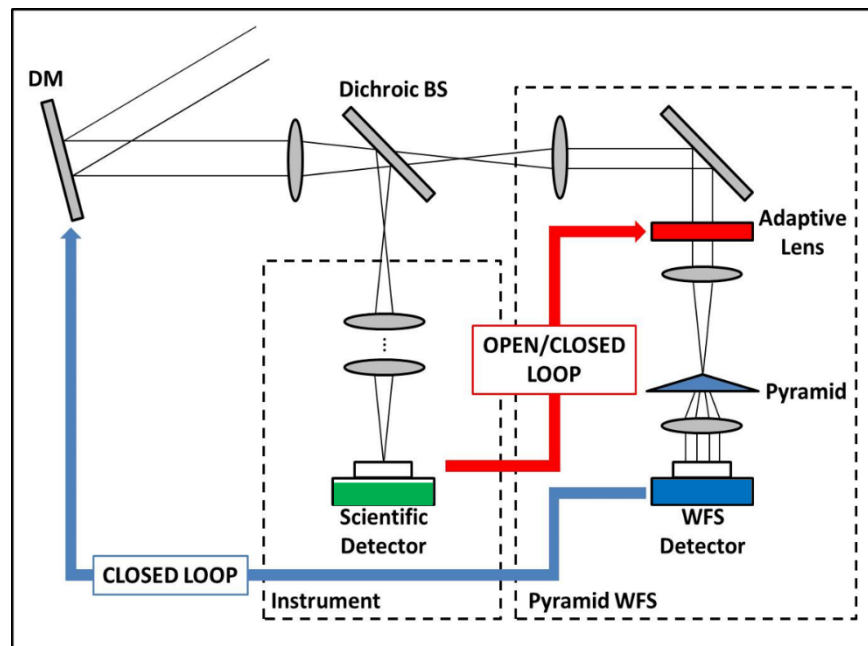


Figure 2: optical scheme of a possible astronomical instrument equipped with AO, with two channels: a scientific one, reaching the science detector (green), and a sensing one, reaching the P-WFS and the WFS detector (blue). After closing the loop, we obtain a high Strehl Ratio PSF (green) on the science path, while a degraded one (blue) on the sensing one. If a MAL (red) is inserted in the WFS channel, it allows to provide a high strehl PSF (red) also to the sensing channel and thus exploit the P-WFS characteristics. [PSF are just pictorial representations.]

To estimate the improvement we are envisaging, we consider the plot adapted from [4] (Figure 3), where the magnitude gain of the P-WFS it is plotted as a function of the SH-WFS SR with respect to the obtainable SR for different  $D/r_0$ . Since the SH-WFS does not have any gain connected to the shrinking of the PSF, we can use this same plot to retrieve the pyramid gain in terms of magnitudes for different SRs. If we consider an 8 meter telescope with P-WFS working at visible wavelength (therefore with  $D/r_0=40$ ), for an aberration of 0.2 waves rms (an NCPA valued retrieved from simulations of a realistic case [15]), the Marechal approximation  $SR = e^{-(2\pi\sigma)^2}$  will give us a SR of 0.2. If we would be able to push down the NCPA to 0.1 waves, we could achieve a SR 0.67. This NCPA reduction would hence translate in an improvement of 0.7 mag in star magnitude (or a higher SNR), making the implementation of a NCPAs correction system of primary importance, especially for the exploitation of faint objects as reference stars.

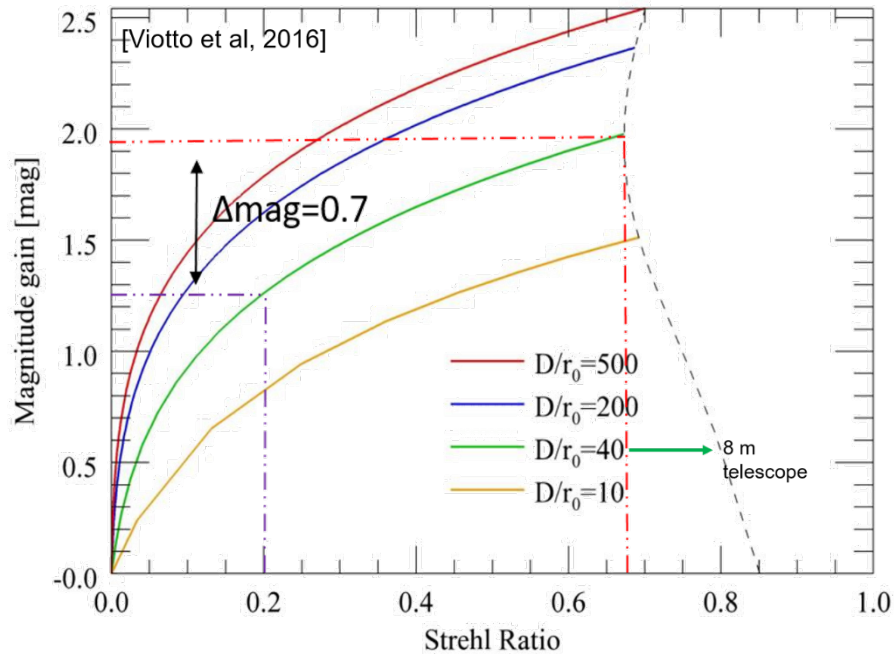


Figure 3: gain in limiting magnitude of 0.7 Mag, achievable for an 8 m telescope, if aberrations of the system are reduced from 0.2 to 0.1 waves rms. Dashed-line shows the maximum SR achievable for that corrected radial order as from Noll 1976. Plot adapted from Viotto et al, 2016.

#### 4. EXPERIMENTAL SETUP CHARACTERIZATION

To demonstrate the correction of NCPAs we realized a laboratory test-bench using off-the-shelf components and three custom deformable elements realized by Dynamics Optics, two MALs and one DM. The test-bench, shown in Figure 4 simulates the P-WFS based AO system of a telescope, similarly to the concept defined in Section 3.

A fiber-coupled LED collimated source reaches a 32-actuators piezoelectric DM, which mimics the adaptive secondary mirror of the telescope and is the pupil of the optical system. In place of the dichroic, a beam splitter (BS 1) re-directs part of the beam to the scientific channel, consisting in two arms separated by a second beam-splitter (BS 2): the imaging channel with a camera and a SH-WFS for a quantitative evaluation of the WFE residuals. The rest of the light is directed to the sensing channel, where a Keplerian telescope is used to collimate again the beam to the MAL pupil size and then other components allow the beam to reach the P-WFS. The MAL used for NCPA correction (MAL\_corr in the figure) is introduced in the intermediate optical plane conjugated to the DM (which, we recall, is the pupil of the system). Also, a second MAL (MAL\_ncp in the figure) can be inserted in front of the correcting one, in order to simulate NCPAs by introducing calibrated low-order aberrations in the system.

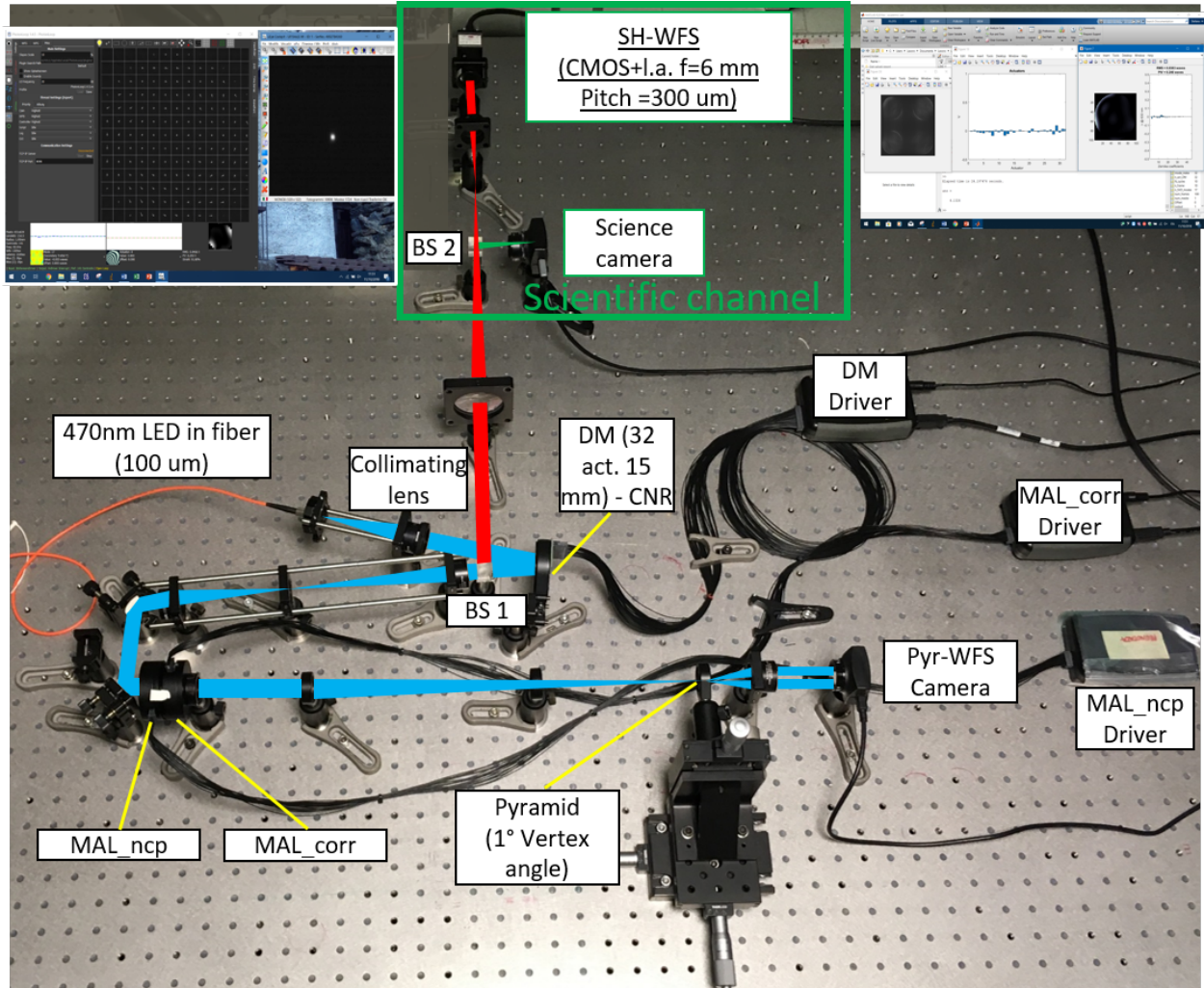


Figure 4: test-bench setup realized at CNR-INF premises in Padova, to simulate the P-WFS based AO system of a telescope, where a custom DM simulates the adaptive secondary of a telescope, and a beam-splitter separates the beam in the scientific channel and the sensing channel. In the scientific path a SH-WFS is introduced to evaluate quantitatively the level of wavefront correction. The MALs used to introduce (MAL\_ncp) and to compensate (MAL\_corr) the NCPAs are placed in the sensing channel.

#### 4.1. NCPAs generation

Our NCPA generator, MAL\_ncp has been characterized and calibrated on a separate optical setup to generate the following sets of low order aberrations with different amplitudes, recalling that astigmatism is one of the most common NCPA, being introduced by the dichroic filter:

- A. best flat: 20 nm rms
- B. astigmatism only : 100, 200 (B2), 400 (B3), 900 nm rms
- C. combination of aberrations up to 3<sup>rd</sup> radial order (defocus, astigmatism, coma, trefoil): 100, 200 (C2) nm rms

The calibration in a separate setup also allowed us to determine the MAL stability over time and the reproducibility of the aberrations, which is fundamental for its use in a real AO setup, which varies from different configurations. In a lab controlled environment it has been measured to be lower than 15 nm rms. Also, it should be noticed that the main contributor is the defocus term, clearly connected with temperature variation (a few degrees °C).

We also measured its influence functions and SVD modes and obtained its control matrix.

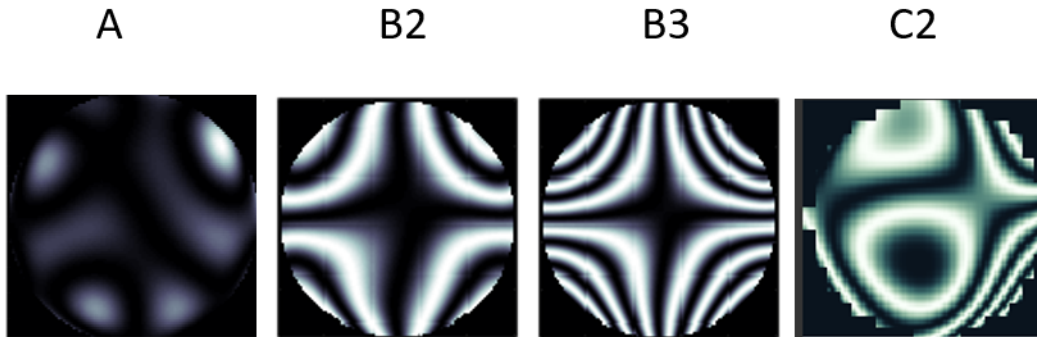


Figure 5: MAL\_ncp residual WFE when flattened (case A: 20 nm rms), generation of astigmatism (case B2: 200 nm rms and case B3: 400 nm rms), generation of mixed aberrations (case C2: 200 nm rms)

#### 4.2. Loops on the test-bench and NCPAs correction strategies

The test bench foresees three loops:

1. DM is working in closed-loop on P-WFS (25Hz). The influence function was computed with a larger fiber (representing static modulation) and 25 modes. Both MALs (MAL\_ncp and MAL\_corr) are in the optical path and active in their best flat configuration. The WF on the sensing arm reaches the lowest achievable error in this setup, of the order of 12 nm rms, considering 16 SVD modes, shown in Figure 6.



Figure 6: Residual wavefront aberration on the P-WFS arm, after closing the loop with the DM, while keeping the two MALs activated in their best flat shape.

2. DM MAL\_corr is working in open loop looking at the PSF on the “scientific” camera, while keeping the loop#1 closed and thus maintaining an optimal image on the pyramid tip. In this way, essentially, the MAL\_corr shape is varied to improve the PSF with a dedicated algorithm and the DM essentially counter-correct all aberrations introduced by the MAL, in order to minimize the P-WFS residual. We recall that the goal is to obtain the best achievable WF residual (thus minimum NCPA) simultaneously both on Scientific camera and on P-WFS.
3. DM MAL\_corr is working in closed loop on the SH-WFS at 2.5 Hz (we recall it is located in the scientific path), while keeping the loop#1 closed (faster) and thus maintaining an optimal image on the pyramid tip. In this way, essentially, MAL shape is varied by the loop to reduce WF residuals on the SH-WFS and the DM essentially compensates all aberrations introduced by the MAL, in order to minimize the P-WFS residual. We recall that the goal is to obtain the best achievable WF residual (thus minimum NCPA) both on SH-WFS and on P-WFS.

Except minor NCPAs, we can also assume that both loop#2 and loop#3, although optimized on scientific camera and SH-WFS respectively, minimize WFE in the scientific path and thus both elements simultaneously.

Loop#2 is a realistic case in an astronomical instrument while loop #3 is used to quantify the WFE residuals.

## 5. RESULTS

We have applied the NCPAs generated with MAL\_ncp, for all cases presented in Section 4.1 and we have recorded the best results achievable on the scientific channel with both technique: sensorless algorithm based on the edges sharpness, using loop #2 and closed loop on SH-WFS using loop#3, while keeping in both cases a low WFE residual on the sensing arm with loop#1.

We report in Figure 7 the obtained results on the scientific channel and on the sensing channel, for the selection of introduced NCPAs (applied through MAL\_ncp) highlighted in Section 4.1. We show visually and quantitatively (in nm rms) the WFE residual on SH-WFS before (1) and after (2) applying the correction with the MAL\_corr commanded in closed-loop #3. The residual obtained range between 20 and 28 nm rms, without a dependency neither from the amplitude of the introduced NCPA nor the combination of the modes. We then display qualitatively the PSF on the scientific channel, before (3) and after (4) applying the correction with the MAL\_corr, as per loop #2. For a real quantification of PSF improvement, e.g. in Strehl Ratio, we are expecting to repeat the test with a resolved image. We also show visually and quantitatively (in nm rms) the WFE residual on the P-WFS (5), obtained when loop#3 is active. They are always below 20 nm rms. We recall that P-WFS WFE is 12 nm, with loop #1 closed and both MALs static and at their best flat.

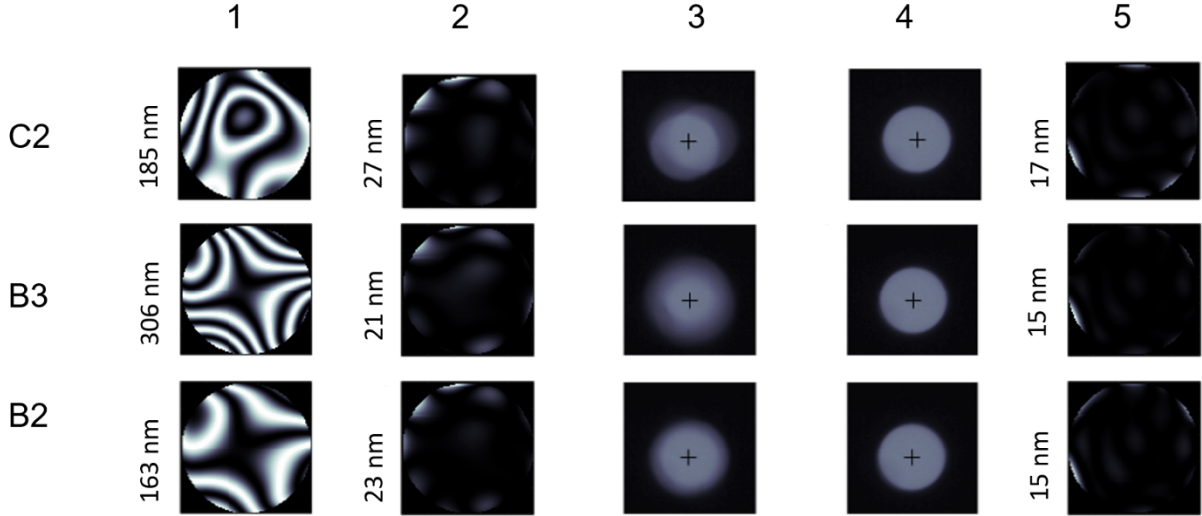


Figure 7: Different lines refer to the cases presented in Figure 5, C2, C3 and B2. We present the WFE residuals (in nm rms) measured on the scientific channel SH-WFS, when applying the NCPA (1) and after correcting them (2) and the ones obtained on the sensing channel P-WFS after the correction (5). We also show qualitatively the PSF images on the scientific channel camera, before (3) and after (4) the correction.

## 6. CONCLUSIONS

NCPAs have been produced by means of a second MAL (MAL\_ncp), to simulate mixed polynomials typical rms values obtained at 8-m telescopes and only astigmatism, which is the main aberration introduced by the dichroic, one of the main contributor to NCPAs in AO astronomical systems.

MAL\_corr has proved able to correct aberrations, maintaining a low WFE on the pyramid (below 20 nm) while the DM could compensate the NCPA in the scientific channel. The latter has been verified using as reference both the PSF in the camera (using a sensorless optimization algorithm) and a SH-WFS, to evaluate the WFE residuals. Further investigations are needed to assess stability over time and temperature of the MAL, chromatism introduced by the MAL, obtain resolved images, prove the robustness of the algorithm for PSF sharpening and WFE residuals correlation with input aberrations.

## Bibliography

- [1] Ragazzoni, R. "Pupil plane wavefront sensing with an oscillating prism", *J. Modern Opt.* 43, 289-293 (1996).
- [2] S. Esposito *et al.*, "First Light Adaptive Optics System for Large Binocular Telescope," *Adapt. Opt. Syst. Technol. II. Ed. by Wizinowich*, pp. 164–173, 2003.
- [3] R. Ragazzoni and J. Farinato, "Sensitivity of a pyramidal wave front sensor in closed loop adaptive optics," *Astron. Astrophys.*, vol. 350, pp. 23–26, 1999.
- [4] V. Viotto, R. Ragazzoni, M. Bergomi, D. Magrin, and J. Farinato, "Expected gain in the pyramid wavefront sensor with limited Strehl ratio," vol. 100, pp. 4–9, 2016.
- [5] F. Rigaut, "Astronomical Adaptive Optics," *Publ. Astron. Soc. Pacific*, vol. 127, no. 958, pp. 1197–1203, 2015.
- [6] R. Davies and M. Kasper, "Adaptive Optics for Astronomy," pp. 1–47, 2012.
- [7] J.-F. Sauvage, T. Fusco, G. Rousset, and C. Petit, "Calibration and Pre-Compensation of Non-Common Path Aberrations for extreme Adaptive Optics," *JOSA Vol. 24, Issue 8*, pp. 2334-2346, 2007.
- [8] A. Vigan, M. N'Diaye, K. Dohlen, J.-F. Sauvage, J. Milli, G. Zins, C. Petit, Z. Wahhaj, F. Cantalloube, A. Caillat, A. Costille, J. Le Merrer, A. Carlotti, J.-L. Beuzit and D. Mouillet "Calibration of quasi-static aberrations in exoplanet direct-imaging instruments with a Zernike phase-mask sensor II . Concept validation with ZELDA on VLT / SPHERE," *Astron. Astrophys.*, vol. 692, A11, 2019.
- [9] A. Vigan, M. N'Diaye, K. Dohlen, J. Milli, Z. Wahhaj, J.-F. Sauvage, J.-L. Beuzit, R. Pourcelot, D. Mouillet, G. Zins "On-sky compensation of non-common path aberrations with the ZELDA wavefront sensor in VLT/SPHERE," *SPIE*, 2018.
- [10] D. Magrin, P. Favazza, S. Bonora, M. Quintavalla, M. Bergomi, R. Ragazzoni, "Multi-actuator adaptive lens in astronomy: in lab test results", *Proc.SPIE*, 2018
- [11] S. A. Moosavi, M. Quintavalla, J. Mocchi, R. Muradore, H. Saghafifar, and S. Bonora, "Improvement of coupling efficiency in free space optical communication system with multi actuator adaptive lens," *Opt. Lett.*, 2018.
- [12] M. Negro, M. Quintavalla, J. Mocchi, A.G. Ciriolo, M. Devetta, R. Muradore, S. Stagira, C. Vozzi, S. Bonora "Fast stabilization of a high-energy ultrafast OPA with adaptive lenses," *Sci. Rep.*, vol. 8, no. 1, pp. 4–9, 2018.
- [13] S. Bonora, Y. Jian, P. Zhang, A. Zam, E.N. Pugh, Jr., R.J. Zawadzki, M.V. Sarunic, "Wavefront correction and high-resolution in vivo OCT imaging with an objective integrated multi-actuator adaptive lens," *Opt. Express*, vol. 23, no. 17, pp. 21931–21941, 2015.
- [14] M. Quintavalla, J. Mocchi, R. Muradore, A. J. Corso, and S. Bonora, "Adaptive optics on small astronomical telescope with multi-actuator adaptive lens," in *Proceedings Volume 10524, Free-Space Laser Communication and Atmospheric Propagation XXX; 1052414 (2018)*, 2018.
- [15] D. Vassallo, J. Farinato, J.-F. Sauvage, T. Fusco, D. Greggio, E. Carolo, V. Viotto, M. Bergomi, L. Marafatto, A. Baruffolo, M. De Pascale, "Validating the phase diversity approach for sensing NCPA in SHARK-NIR, the second-generation high-contrast imager for the Large Binocular Telescope", *Proc. SPIE*, 2018